Supplementary data for

Electrochemical and Mechanistic Study of Superoxide Scavenging by Pyrogallol in *N*,*N*-Dimethylformamide through Proton-Coupled Electron Transfer

Tatsushi Nakayama [1]*, Ryo Honda [2], Kazuo Kuwata [2], Shigeyuki Usui [1], and Bunji Uno [3]

[1] Department of Pharmacy, Gifu Pharmaceutical University, 1-25-4 Daigaku-nishi, Gifu 501-1196, Japan

[2] United Graduate School of Drug Discovery and Medical Information Sciences, Gifu University, 1-1 Yanagido, Gifu 501-1193, Japan

[3] Faculty of Pharmacy, Gifu University of Medical Science, 4-3-3 Nijigaoka, Kani, Gifu 509-0923, Japan

* Correspondence: tnakayama@gifu-pu.ac.jp

Table of contents

Pages S6-S13 Table S6: Calculated geometries of complexes (PRC, TS, and PC) formed along the PCET between PyH_3 and $O_2^{\bullet-}$

Table S1. CV parameters

Working Electrode Planar Radius 1.0 mm diameter			
Geometry Spherical (Hemispherical)[1]	Diffusion Semi-infinite 1D	Temperature 298.3 K	
Charge Transfer Reaction			
$O_2 + e^- \leftrightarrow O_2^{\bullet-}$	Redox Potential (V vs Fc^+/Fc)	Coefficient	Kinetics (cm s^{-1})
	$E = -1.284$	$\alpha = 0.005$	$k_s = 0.00927$
Species			
	Diffusion Coefficient (cm^2 s^{-1})	Initial Concentration (mol L^{-1})	
O_2	$4.76 \pm 0.24 \times 10^{-5}$	0.0048	
$O_2^{\bullet-}$	$2.15 \pm 0.24 \times 10^{-5}$	0	

[1]Operating conditions were spherical diffusion (to mimic edge diffusion to the disk)
[2]Digielch 4.5 ElchSoft inc. (Digital CV Simulation Software)

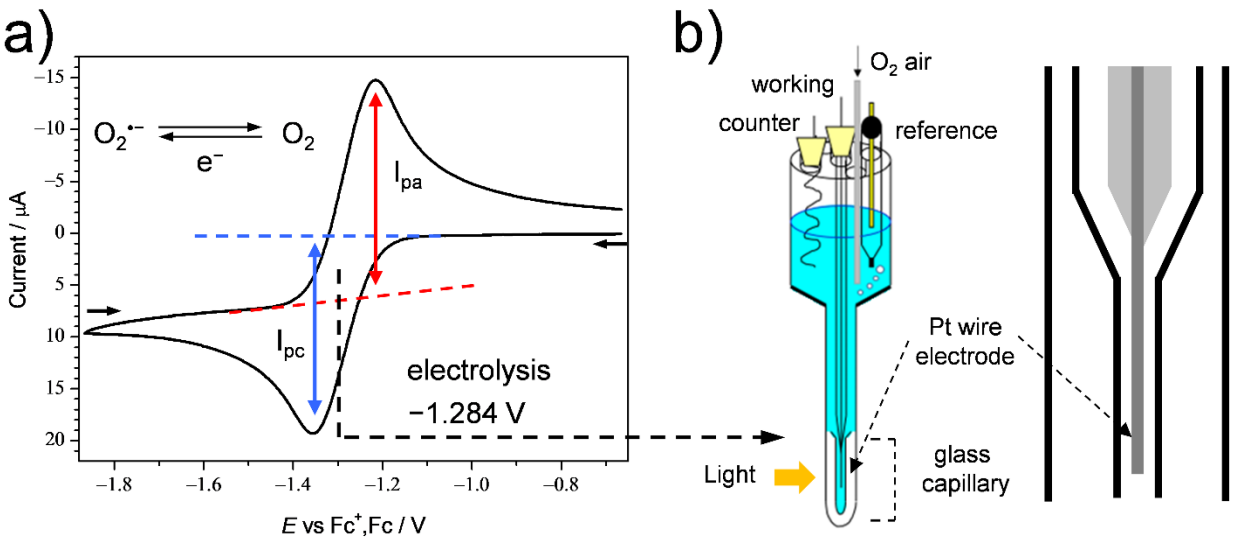

Figure S1. In situ electrolytic ESR spectral system. (a) Cyclic voltammograms of $O_2/O_2^{\bullet-}$ for potential determination. (b) In situ ESR system, composed of an electrochemical ESR cell with a glass small tip, air tube for O_2 bubbling, and three electrode system using a 0.5-mm-diameter straight Pt wire sealed in a glass capillary as working electrode.

Table S2. ΔG^o values (kJ mol^{-1}) for the PCET reaction between $O_2^{\bullet-}$ and the compounds ($CatH_2$, PyH_3, and $MoCatH_2$) in acetonitrile, calculated using (U)B3LYP/PCM/6-311+G(3df,2p) methods.

	PT1	PT2	PT3	PT4	ET1	ET2	ET3	PCET	2PCET
$CatH_2$	19.3	-365.4	378.5	-78.9	408.0	23.2	-434.2	-55.7	-36.3
PyH_3	17.8	-360.2	358.9	-67.9	406.4	28.3	-398.5	-39.5	-21.7
$MoCatH_2$	46.0	-336.5	380.6	-92.5	396.1	13.4	-459.6	-79.0	-32.9

Table S3. ΔG^{o} values (kJ mol^{-1}) for the PCET reaction between $O_2^{\bullet-}$ and the compounds ($CatH_2$, PyH_3, and $MoCatH_2$) in dimethyl sulfoxide, calculated using (U)B3LYP/PCM/6-311+G(3df,2p) methods.

	PT1	PT2	PT3	PT4	ET1	ET2	ET3	PCET	2PCET
$CatH_2$	19.8	-358.5	385.8	-78.3	400.9	22.5	-441.5	-55.7	-35.9
PyH_3	18.2	-353.3	353.1	-67.2	399.3	27.6	-392.6	-39.5	-21.2
$MoCatH_2$	46.0	-329.9	374.4	-92.0	389.0	13.0	-453.5	-79.0	-32.9

Table S4. ΔG^{o} values (kJ mol^{-1}) for the PCET reaction between $O_2^{\bullet-}$ and the compounds ($CatH_2$, PyH_3, and $MoCatH_2$) in water, calculated using (U)B3LYP/PCM/6-311+G(3df,2p) methods.

	PT1	PT2	PT3	PT4	ET1	ET2	ET3	PCET	2PCET
$CatH_2$	20.3	-349.5	378.1	-77.5	391.6	21.7	-434.0	-55.8	-35.4
PyH_3	18.8	-344.3	345.5	-66.2	390.0	26.8	-384.9	-39.4	-20.5
$MoCatH_2$	46.0	-321.4	366.4	-91.5	379.9	12.4	-445.5	-79.0	-33.0

Table S5. ΔG^{o} values (kJ mol^{-1}) for the PCET reaction between $O_2^{\bullet-}$ and the compounds ($CatH_2$, PyH_3, and $MoCatH_2$) in vacuum, calculated using (U)B3LYP/PCM/6-311+G(3df,2p) methods.

	PT1	PT2	PT3	PT4	ET1	ET2	ET3	PCET	2PCET
$CatH_2$	-60.4	-1385.1	1279.3	-159.8	1444.0	119.3	-1319.8	-40.4	-100.9
PyH_3	-66.9	-1374.7	1212.8	-170.9	1437.1	129.3	-1254.4	-41.6	-108.5
$MoCatH_2$	-6.0	-1323.8	1241.7	-180.3	1417.8	100.0	-1322.1	-80.3	-86.4

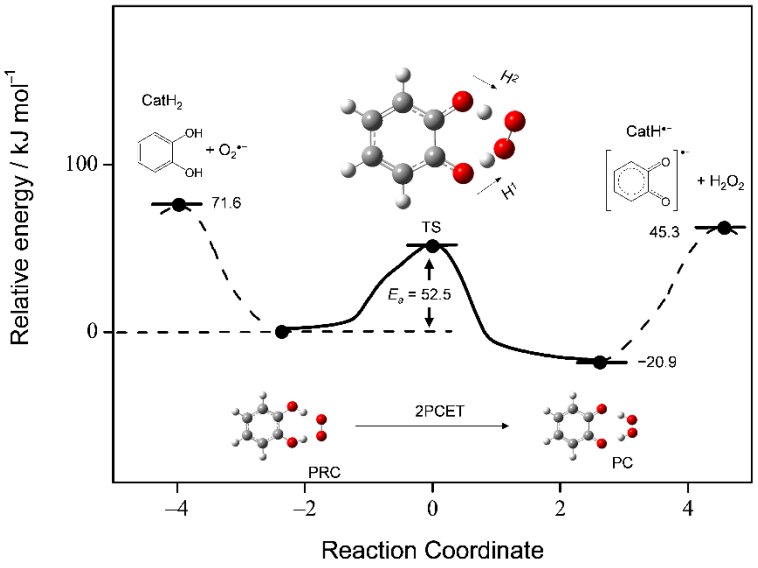

Figure S2. Energy profile (kJ mol^{-1}) along the IRC of the 2PCET between $CatH_2$ and $O_2^{\bullet-}$ in DMF with structures of FRs ($CatH_2$, $O_2^{\bullet-}$), PRC ($CatH_2$–$O_2^{\bullet-}$), TS, PC ($Cat^{\bullet-}$–H_2O_2), and FPs ($Cat^{\bullet-}$, H_2O_2), calculated using DFT-(U)B3LYP/PCM/6-311+G(3df,2p) method.

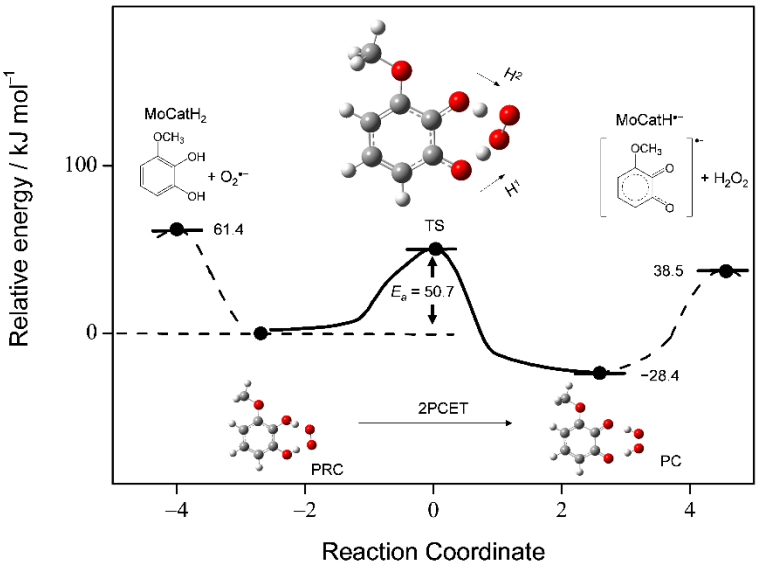

Figure S3. Energy profile (kJ mol^{-1}) along the IRC of the 2PCET between $MoCatH_2$ and $O_2^{\bullet-}$ in DMF with structures of FRs ($MoCatH_2$, $O_2^{\bullet-}$), PRC ($MoCatH_2$–$O_2^{\bullet-}$), TS, PC ($MoCat^{\bullet-}$–H_2O_2), and FPs ($MoCat^{\bullet-}$, H_2O_2), calculated using DFT-(U)B3LYP/PCM/6-311+G(3df,2p) method.

Table S6. Optimized geometry of complexes (PRC, TS, and PC) formed along the 2PCET between PyH_3 and $O_2^{\bullet-}$ calculated using DFT-(U)B3LYP/PCM/6-311+G(3df,2p) in DMF.

Center Number	Atomic Number	Coordinates (Angstroms) X	Y	Z
-PRC----------				
1	6	1.181897	-1.84196	-0.06596
2	6	0.06826	-1.03843	0.202336
3	6	0.221736	0.356216	0.22686
4	6	1.486161	0.908188	-0.01953
5	6	2.592423	0.110095	-0.27751
6	6	2.426881	-1.27204	-0.29633
7	1	1.047691	-2.91533	-0.08233
8	1	3.554319	0.569762	-0.45842
9	1	3.277846	-1.90975	-0.49659
10	8	1.616241	2.268443	0.016273
11	1	0.733112	2.622022	0.203096
12	8	-0.76731	1.237787	0.548122
13	1	-1.66049	1.069864	0.077844
14	8	-1.11312	-1.64656	0.472696
15	1	-1.92325	-1.09988	0.236284
16	8	-3.30296	-0.42191	-0.26998
17	8	-3.04453	0.853596	-0.5295
-TS----------				
1	6	1.481072	0.891171	0.059877
2	6	0.201635	0.388281	-0.25156
3	6	-0.02594	-1.03381	-0.30444
4	6	1.092044	-1.87109	-0.03328
5	6	2.330801	-1.34326	0.259256
6	6	2.542867	0.045301	0.310444
7	1	0.936235	-2.94151	-0.06901
8	1	3.163025	-2.00692	0.456686
9	1	3.516047	0.456834	0.539721
10	8	-1.19241	-1.50821	-0.5994

11	1	-2.23727	-0.9208	0.281739
12	8	-0.73629	1.294887	-0.54229
13	1	-1.73773	1.015622	-0.32236
14	8	-2.94759	-0.39799	0.81965
15	1	0.79236	2.643126	-0.10118
16	8	1.653703	2.246055	0.095463
17	8	-3.04835	0.777028	0.098148

-PC----------

1	6	-1.6067	0.918052	-0.0358
2	6	-0.25561	0.405283	-0.01653
3	6	-0.06345	-1.05977	0.029501
4	6	-1.24505	-1.86692	0.065874
5	6	-2.49639	-1.30811	0.049218
6	6	-2.69765	0.096077	-0.00316
7	1	-1.114	-2.94054	0.103607
8	1	-3.36738	-1.95084	0.075757
9	1	-3.696	0.511511	-0.01592
10	8	1.099258	-1.56706	0.037436
11	1	2.574259	-0.86554	-0.27943
12	8	0.696442	1.246655	-0.0428
13	1	2.349146	1.007136	0.296185
14	8	3.42224	-0.37527	-0.45585
15	1	-0.80768	2.60238	-0.09488
16	8	-1.72331	2.270097	-0.08428
17	8	3.286694	0.741594	0.467989
